Structural control on the rheological behavior of binary P-Se supercooled liquids

Bing Yuan [a], Bruce Aitken [b], Sabyasachi Sen [a,*]

[a] Department of Materials Science & Engineering, University of California at Davis, Davis, CA 95616, USA
[b] Science & Technology Division, Corning Inc., Corning, NY 14831, USA

ABSTRACT

The link between the atomic structure and the shear relaxation behavior of P_xSe_{100-x} ($0 \leq x \leq 25$) supercooled liquids is investigated using Raman spectroscopy and parallel plate rheometry. The P atoms in these glasses form $Se=P(Se_{1/2})_3$, $P(Se_{1/2})_3$ and $_{2/2}SeP-PSe_{2/2}$ units, which serve as cross-linkers of the $[Se]_n$ chain segments. The frequency dependence of the storage and loss moduli as well as the relaxation spectra $H(\tau)$ indicate that liquids with $>85\%$ Se are characterized by the coexistence of a slow and a fast relaxation process corresponding to bond scission/renewal and Se chain segmental motion, respectively. On the other hand, liquids with $\leq 85\%$ Se display only the bond scission/renewal process. The $H(\tau)$ spectra suggest that the relaxation-time τ distribution for Se chain dynamics is a sensitive function of the chain length, while that for bond scission/renewal is controlled by the variety of bond types and structural moieties involved.

1. Introduction

The rheological behavior of supercooled glass-forming liquids is intimately linked to their viability for various processing techniques [1, 2]. Thus, a fundamental understanding of the structural control on the rheological behavior of glass-forming liquids is of paramount importance in the optimization of the corresponding processing parameters. Comprehensive and systematic studies in this direction have recently been carried out on a variety of binary chalcogenide glass-formers in the As-Se, Ge-Se, Se-Te and As-S systems [3–7]. While the structure of glassy/liquid Se consists primarily of two coordinated Se atoms forming polymeric $[Se]_n$ chains [8], the addition of Ge or As results in progressive cross-linking of these chains and a concomitant shortening of the segmental chain length [9–11]. Rheological studies of supercooled Se-rich liquids using small angle oscillatory shear (SAOS) have shown the existence of a slow and a fast relaxation process with widely different timescales and relaxation moduli. The slow and fast processes were shown to correspond to bond scission/renewal and segmental motion of Se chains, respectively [12,13]. Progressive shortening of the Se chain length with increasing Ge/As concentration leads to an increase in the timescale of the segmental chain motion, as this dynamical process becomes increasingly dependent on and thus temporally coupled to the bond scission/renewal [3,4]. Although all slow relaxation processes correlate to the bond scission/renewal event, some variations still exist in between systems because different chemical bonds/interactions are involved in different structural environments. For instance, the bond

scission/renewal process in the binary Se-Te system involves not only the possible Se-Se, Se-Te, and Te-Te bonds, but also the strong secondary bonding interactions between adjacent chains, resulting in a much broader relaxation time distribution when compared with the slow relaxation process in pure Se [6]. This structural evolution of the viscoelastic relaxation ultimately results in the disappearance of the segmental chain motion across all binary systems as the Se chain segments become too short (≤ 3 to 5 Se atoms) to sustain the segmental motion [3]. At this point the shear relaxation of these liquids is entirely controlled by the bond scission-renewal dynamics. While segmental chain motion is expected to be a function of the effective chain length, the bond scission/renewal is expected to be controlled by the bond types associated with the various structural moieties in the liquid. In fact, an analysis of the relaxation spectrum derived from the frequency dependent shear modulus data has shown that, compared to pure Se, binary Se-Te liquids with copolymeric $[Se,Te]_n$ chains display a broader distribution of the bond scission/renewal timescales [6]. This result was hypothesized to be indicative of the fact that, unlike pure Se consisting of only Se-Se bonds, bond scission in Se-Te alloys involves a variety of bond types, including Se-Se, Se-Te and Te-Te, as well as the secondary bonds involving Te atoms. Here we extend such studies to the supercooled liquids in the binary P-Se system to systematically investigate the effect of a wide variety of different bond types, structural moieties and connectivity on the viscoelastic relaxation behavior.

The P-Se system exhibits an extensive glass formation range which can be divided into two regions, the Se-rich region with $0 \leq x \leq 54$ and
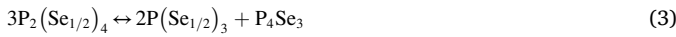
---

* Corresponding author.
  E-mail address: sbsen@ucdavis.edu (S. Sen).

P-rich regions with $64 \leq x \leq 84$. The narrow composition window in between these two regions is centered on the P_4Se_3 stoichiometry, which displays high crystallization tendency [14]. The composition-dependent structural evolution in the Se-rich and P-rich glass formation regions has been extensively investigated by Raman scattering, and solid state ^{77}Se and ^{31}P nuclear magnetic resonance (NMR) spectroscopy [15–21]. These studies have indicated that the structure of P-Se glasses with P content below 30 atom% consists primarily of Se=P(Se$_{1/2}$)$_3$ tetrahedral units and P(Se$_{1/2}$)$_3$ pyramidal units linked by [Se]$_n$ chains. The relative fraction of the [Se]$_n$ chains decreases with increasing P content and the structure changes to a polymeric network consisting predominantly of $_{2/2}$SeP-PSe$_{2/2}$ and some P(Se$_{1/2}$)$_3$ units that are connected via short Se-Se segments. Finally, at P contents of ≥ 45 atom% a significant amount of embedded P_4Se_3 molecules appear in these glasses. Previous variable-temperature ^{31}P and ^{77}Se NMR spectroscopy studies [22–24] showed the presence of two types of dynamical processes in P-Se liquids within this composition range: at low P contents ($\leq 25\%$) the dynamics involve Se site exchange between Se-bonded and P-bonded Se via reaction 1 (see below), while at higher P contents ($\geq 30\%$) the process involves the interconversion between different P sites as represented by Eqs. (2) and (3) below:

$$P\left(Se_{1/2}\right)_3 + Se \leftrightarrow Se = P\left(Se_{1/2}\right)_3 \tag{1}$$

$$P_2\left(Se_{1/2}\right)_4 + Se \leftrightarrow 2P\left(Se_{1/2}\right)_3 \tag{2}$$

$$3P_2\left(Se_{1/2}\right)_4 \leftrightarrow 2P\left(Se_{1/2}\right)_3 + P_4Se_3 \tag{3}$$

Therefore, the liquids in the P-Se system with their rich structural complexity lend themselves as ideal candidates for an exploration of the effects of the variety in bonding and structural moiety and connectivity on the shear relaxation behavior. Here we investigate such effects in a detailed rheological study of the shear relaxation behavior of binary P-Se supercooled liquids with ≤ 25 atom% P using small amplitude oscillatory shear (SAOS) measurements. The glass structure was characterized using Raman spectroscopy and correlations between glass structure and shear relaxation behavior are discussed in detail.

2. Experimental

2.1. Sample preparation and characterization

Binary P_xSe_{100-x} glasses with $x = 5, 10, 15, 20, 25$ were synthesized in ~12g batches using the conventional melt-quench method. Elemental red phosphorus (Spectrum, 99.999%) and selenium (Alfa Aesar, 99.999%) were mixed together in stoichiometric ratios and subsequently flame-sealed in evacuated (10^{-4} Torr) quartz ampoules. The ampoules were then sealed and placed in a rocking furnace, slowly heated to 923K over 13 hours and held at this temperature for 36 h to ensure melt homogeneity. The melts were subsequently quenched to form glass by dipping the ampoules in water.

The glass transition temperature T_g of these P_xSe_{100-x} glasses was measured using a Mettler-Toledo DSC1 differential scanning calorimeter. Approximately 15 mg of powdered glass sample was loaded in a hermetically sealed 40 μL aluminum crucible, and scans were performed at 10 °C/min under a continuously flowing nitrogen environment. T_g was determined to within ± 1 °C as the onset of the glass transition. The unpolarized Raman spectra of all glasses were collected in backscattering geometry with a resolution of 1 cm^{-1}, using a Renishaw 1000 Raman Microscope System equipped with a diode laser operating at a wavelength of 785 nm. Backscattered light was detected using a charge-coupled device cooled at 200 K.

2.2. SAOS parallel plate rheometry

The SAOS and steady shear rheological measurements reported here

were carried out on either an MCR92 or an MCR302 parallel plate rheometer (Anton-Paar) under a constant flow of nitrogen gas, respectively. The temperature is controlled by a Peltier heater (up to 200 °C) in MCR92 and a convection oven (up to 600 °C) in MCR302. In both setups, the upper plate was used to apply strain and measure torque while the bottom plate remained stationary. During each measurement the glass sample was first rapidly heated and trimmed at its softening point to achieve a sandwich geometry between the upper oscillatory plate and lower stationary plate with plate size of 8 mm and 25 mm diameter for the SAOS and the steady shear measurements, respectively, with a gap/sample thickness of ~ 1 mm. At each desired measurement temperature, the samples were allowed to equilibrate for 5 minutes followed by the application of a sinusoidal strain with varying angular frequency ω between 1 to 600 rad/s and the induced torque was recorded to calculate the storage and loss moduli G′and G′′ as a function of ω. Measurements were carried out at multiple temperatures for each sample and master curves of G′(ω) and G′′(ω) were constructed using time-temperature superposition (TTS). All SAOS measurements are done within the predetermined linear viscoelastic range. The viscosity of all supercooled P_xSe_{100-x} liquids was obtained under steady shear condition with samples confined in a ~0.8 mm gap between two plates. At each temperature, the Newtonian viscosity was measured at shear rates $\dot{\gamma}$ ranging between 0.01/s to 100/s and the average viscosity is reported.

3. Results and discussion

The Raman spectra of all P_xSe_{100-x} glasses are shown in Fig. 1. The compositional evolution of these spectra agrees well with those reported on similar compositions in a previous study by Georgiev et al. [15]. The most intense band in these spectra centered at ~ 250 cm^{-1} corresponds to Se–Se stretching mode in [Se]$_n$ [25]. The bands centered at ~ 330 cm^{-1} and 210 cm^{-1} correspond, respectively, to symmetric and asymmetric stretching of P-Se bonds in the pyramidal P(Se$_{1/2}$)$_3$ units. On the other hand, the vibrational modes of the ethylene-like $_{2/2}$SeP-PSe$_{2/2}$ units give rise to the bands located at ~ 185 cm^{-1}, 330-350 cm^{-1} and 370 cm^{-1}. Finally, the broad band centered at ~ 500 cm^{-1} corresponds to the stretching of the P=Se bonds in the Se=P(Se$_{1/2}$)$_3$ tetrahedral units [15]. It is to be noted here that the Raman spectra in Fig. 1 differ from those reported by Georgiev et al. [15] in one important respect. In the present study the 185 cm^{-1} band corresponding to the $_{2/2}$SeP-PSe$_{2/2}$
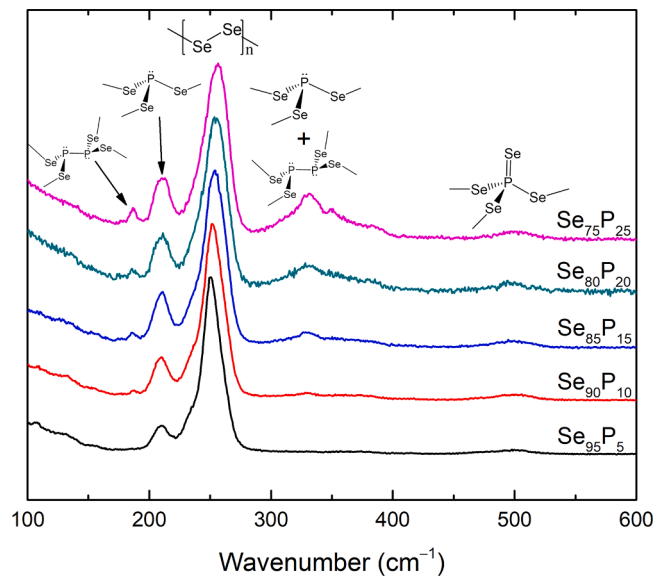

Fig. 1. Unpolarized Raman spectra of P_xSe_{100-x} glasses showing structural assignment of various bands (see text for details). All spectra are normalized to the most intense peak at ~ 250 cm^{-1}.

units appears clearly for the first time in the Raman spectrum of the $P_{15}Se_{85}$ glass, although it can be argued that the first hint of this band can be seen even in the spectrum of the $P_{10}Se_{90}$ glass (Fig. 1). In contrast, this band becomes barely visible for the first time in the Raman spectrum of the $P_{20}Se_{80}$ glass reported by Georgiev et al. [15]. It is unclear whether this difference could stem from the fact that the Raman spectra of Georgiev et al. were collected using a wavelength of 647 nm, which is located close to the optical band gap of amorphous Se and Se-rich chalcogenide glasses. However, a recent study by Bytchkov et al. [16] based on two-dimensional J-resolved ^{31}P magic-angle-spinning nuclear magnetic resonance (NMR) spectroscopy has conclusively shown that the $_{2/2}SeP\text{-}PSe_{2/2}$ units appear in P-Se glasses with >10% P, and a significant fraction (~ 6-7%) of P atoms resides in these units in the $P_{15}Se_{85}$ glass. Therefore, the Raman spectra of P_xSe_{100-x} glasses obtained in the present study (Fig. 1) are indeed consistent with the ^{31}P NMR results of Bytchkov et al. [16].

As expected, the intensities of all bands corresponding to the P-containing structural moieties exhibit a monotonic increase with respect to that the 250 cm^{-1} band with progressive addition of P to Se (Fig. 1). This result demonstrates that addition of P to Se in this composition range results in an increasing degree of structural cross-linking and concomitant shortening of the average length of the $[Se]_n$ chain segments. The increasing structural connectivity and thus rigidity with increasing P content are also evident in the corresponding compositional variation in the T_g (Fig. 2) and viscosity (Fig. 3) of these liquids [15, 26–30]. Besides T_g, the high-temperature viscosity determined in the present study, as well as the previously reported low-temperature viscosity data [30], show that the isothermal viscosity of these liquids monotonically increases with increasing P concentration (Figs. 2,3). These viscosity data over the entire temperature range shown in Fig. 3 are fitted to the MYEGA equation [31,32]:

$$log\ \eta = log_{10}\eta_\infty + \frac{K}{T}\cdot exp\left(\frac{C}{T}\right) \qquad (4)$$

where the parameters $log_{10}\eta_\infty$, K, and C are all treated as fitting variables. The fragility index m, where $m = \frac{d log_{10}\eta}{dT_g/T}|_{T=T_g}$, was subsequently calculated from these fitting parameters using the relation [32]:

$$m = \left(\frac{K}{T_g}\right)\left(1+\frac{C}{T_g}\right)\exp\left(\frac{C}{T_g}\right) \qquad (5)$$

The compositional variation of m thus obtained for these P-Se liquids (Fig. 4) displays a sharp decrease with increasing P content up to 15% P,
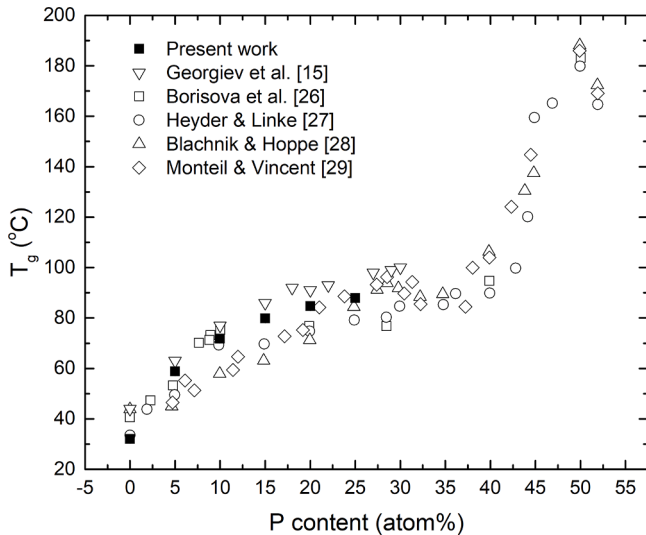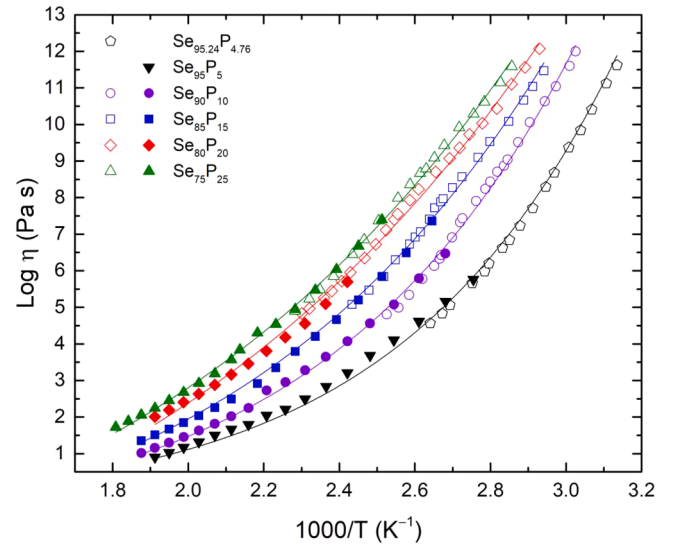

Fig. 3. Temperature dependence of viscosity η of binary P_xSe_{100-x} liquids. Filled symbols correspond to data obtained in the present study, while corresponding open symbols are data taken from a previous study [30]. Solid lines through the datapoints are fits to the MYEGA equation (see Eqn. 4 in text for details). Compositions corresponding to the different symbols are explained in the legend.
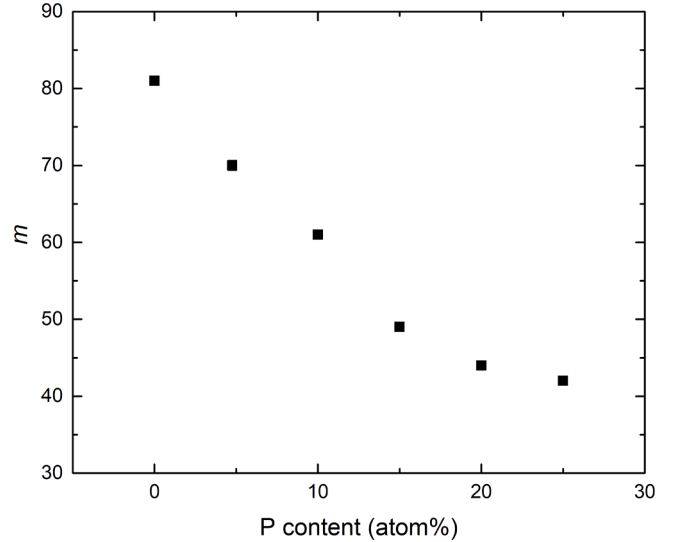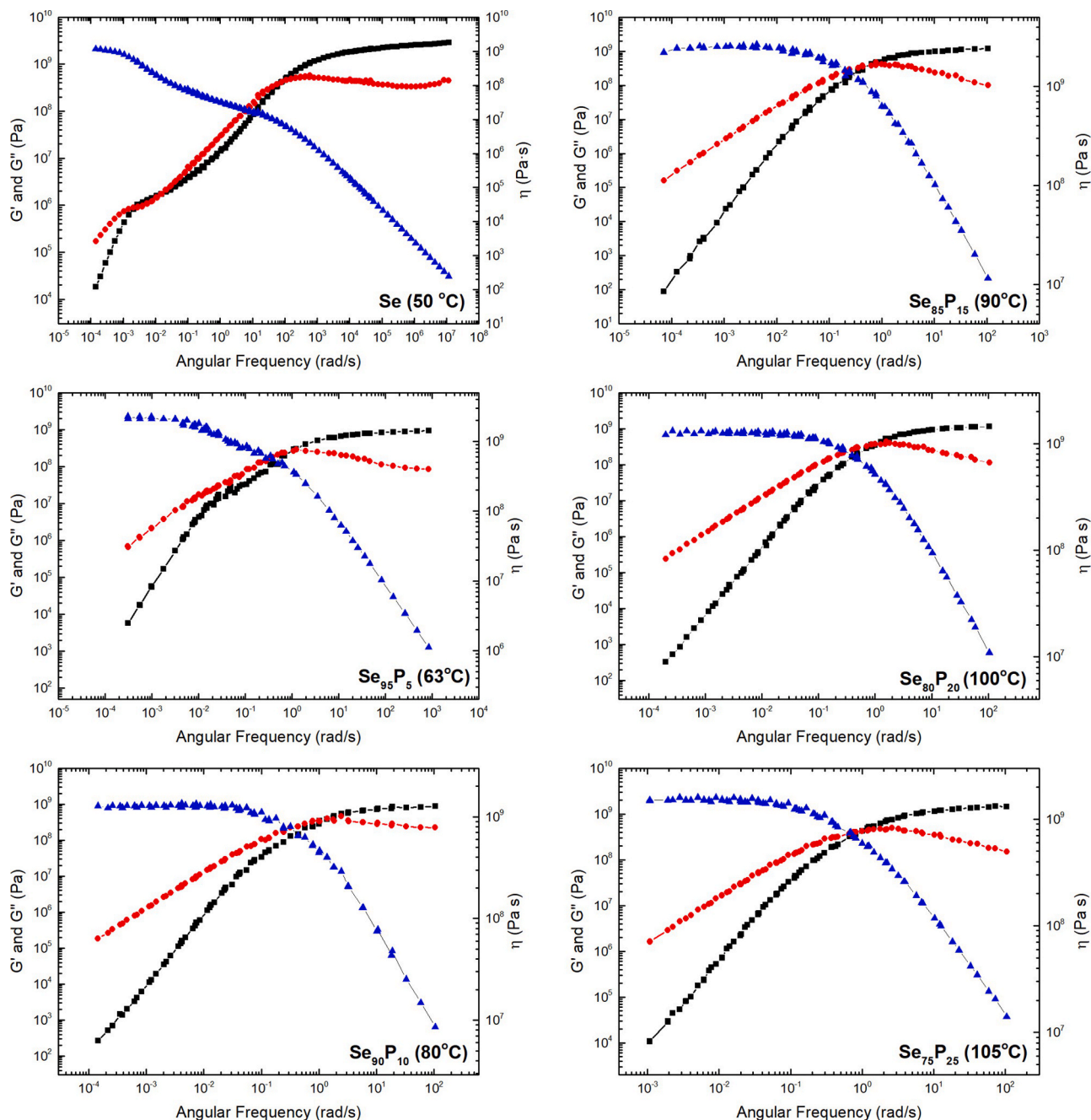

Fig. 4. Composition dependence of fragility index m of P_xSe_{100-x} liquids. Errors are within the size of the symbols. Fragility index for pure Se is taken from Koštál et al. [36].

which is consistent with the rapid lowering of the Se chain conformational entropy upon cross linking with P atoms [3].

The impact of this structural evolution on the rheological behavior is apparent in the experimental master curves of G'(ω) and G(ω) constructed using TTS at nearly iso-viscous (~ 10^9 Pa s) temperatures for all P_xSe_{100-x} supercooled liquids Fig. 5. In the low frequency regime G'(ω) < G''(ω), and both moduli approximately follow the Maxwell scaling of G'(ω) ~ $ω^2$ and G''(ω) ~ ω. On the other hand, in the high-frequency elastic regime G'(ω) approaches its glassy limit G_∞, while G''(ω) decreases with increasing frequency. The corresponding dynamical viscosity $\eta\ (\omega) = \frac{\sqrt{G'^2+G''^2}}{\omega}$ shows a transition from a frequency-independent to a frequency-dependent behavior with increasing ω (Fig. 5). As has been shown in previous studies, the region between the low- and high-

Fig. 2. Composition dependence of T_g of binary P_xSe_{100-x} glasses determined in the present study and reported in the literature.

Fig. 5. Master curves of the frequency dependence of storage modulus G′ (squares), loss modulus G′′ (circles) and viscosity η (triangles) of P_xSe_{100-x} supercooled liquids with the reference temperature listed alongside the composition in each plot. Data for pure Se, included for comparison, are from Zhu et al. [13].

frequency regimes for the Se liquid is marked by two crossovers between G′ and G′′ and two corresponding transitions in the frequency dependence of η (ω) (Fig. 5) [13]. Moreover, at intermediate frequencies G′(ω) displays a linear frequency dependence (Fig. 5). The two crossovers between G′ and G′′ clearly suggest the presence of two relaxation processes in liquid Se with characteristic frequencies marked by the locations of these crossovers, which were assigned in previous studies to the fast segmental chain motion and the slow bond scission/renewal dynamics [12,13]. The initial addition of 5 to 10 at.% P to Se appears to bring the timescales of these dynamical processes closer i.e. increases their temporal coupling to such an extent that the overlapping G′′(ω) peaks for the two processes obscure the low-frequency G′- G′′ crossover (Fig. 5). However, the underlying existence of the two dynamical processes can be clearly observed in the two onsets of the frequency

dependence of η(ω). Furthermore, for these liquids the linear frequency-scaling of G′(ω) at intermediate frequencies is also apparent in Fig. 5. Such a scaling behavior was observed in previous studies to be a characteristic of short chains containing a few molecules in supramolecular polymeric liquids [33,34]. The increased coupling between the chain motion and bond scission/renewal in these P-Se liquids suggests that the rigidity constraints imposed on the mobility of the Se chain segments due to their cross linking with the P atoms can only be overcome successfully via breaking of the constituent P-Se and Se-Se bonds in the structure. Indeed Eqs. (1) and ((2) derived from dynamical NMR studies [22–24] could be interpreted as representing the coupling between Se-Se and P-Se bond scission in the structure. Further increase in the P content (≥ 15 at.% P) results in a single G′-G′′ crossing characteristic of liquids with a single α-relaxation timescale. The disappearance

of the dynamical process corresponding to the fast segmental chain motion is consistent with the cross-linking induced shortening of the Se chain segments in these liquids with $\geq$ 15 at.% P to the point that they can no longer sustain the fast segmental motion.

Further insight into the structural control on the dynamics of these P_xSe_{100-x} liquids can be obtained from the relaxation spectrum i.e. from the distribution of the relaxation times H(τ) in these supercooled liquids. The H(τ) spectrum can be calculated from the G'(ω) and G''(ω) data following Ninomiya and Ferry's method [35],

$$H(\tau) = \frac{G'(a\omega) - G'(\omega/a)}{2\ln a}$$
$$- \frac{a^2}{(a^2-1)^2} \frac{G'(a^2\omega) - G'(\omega/a^2) - 2G'(a\omega) + 2G'(\omega/a)}{2\ln a}\Big|_{1/\omega=\tau}$$

where a is the frequency increment on a logarithmic scale of the measurement. The compositional evolution of the H(τ) spectra for all P-Se supercooled liquids is shown in Fig. 6. Two relaxation processes with overlapping timescale distributions can be immediately recognized in the H(τ) spectra of pure Se and Se-rich compositions with $\leq$10 at.% P. Deconvolution of the H(τ) spectrum of Se shows a broad and intense peak at shorter timescales corresponding to the segmental chain motion and a weaker and narrower peak centered at longer timescales corresponding to bond scission/renewal. The relative peak intensity is determined by the probability of the relaxation mechanism, which

reflects the predominance of the segmental chain motion in Se and P_5Se_{95} liquids. The peak corresponding to bond scission/renewal broadens and becomes more intense with progressive shortening of the Se chain length upon addition of P up to 10 at. %. On the other hand, only one relaxation process is evident in the H(τ) spectra of compositions with 15-25 at.% P. At this point the Se chain segments in the structure are too short to sustain the segmental dynamics and the composition-independent H(τ) spectra are dominated by bond scission/renewal.

The timescale distribution for the segmental chain motion should reflect the associated conformational entropy and, thus, would be a sensitive function of the effective chain length. This idea is borne out in the composition dependence of the corresponding peak full-width-at-half-maximum (FWHM) in the H(τ) spectra in Fig. 6. The FWHM of this peak decreases from $\sim$ 2.0 to $\sim$ 0.8 log units upon increasing the P content from 0 to 10 at.%. On the other hand, the timescale distribution for the bond scission/renewal dynamics is expected to be controlled by the variety of the bond types and structural units. This hypothesis appears to be consistent with the increase in the corresponding peak FWHM from $\sim$ 0.35 to $\sim$ 1.23 log units in the H(τ) spectra Fig. 6) as the P content is increased from 0 to 10 at. % along with the diversity in the bonding and structure, including the appearance of P-Se, P-P and P=Se bonds, as well as $PSe_{3/2}$ pyramids, $Se=P(Se_{1/2})_3$ tetrahedra and ethylene-like $_{2/2}SeP-PSe_{2/2}$ units in addition to the Se-Se bonds in Se chains. The validity of these hypotheses can be further tested by
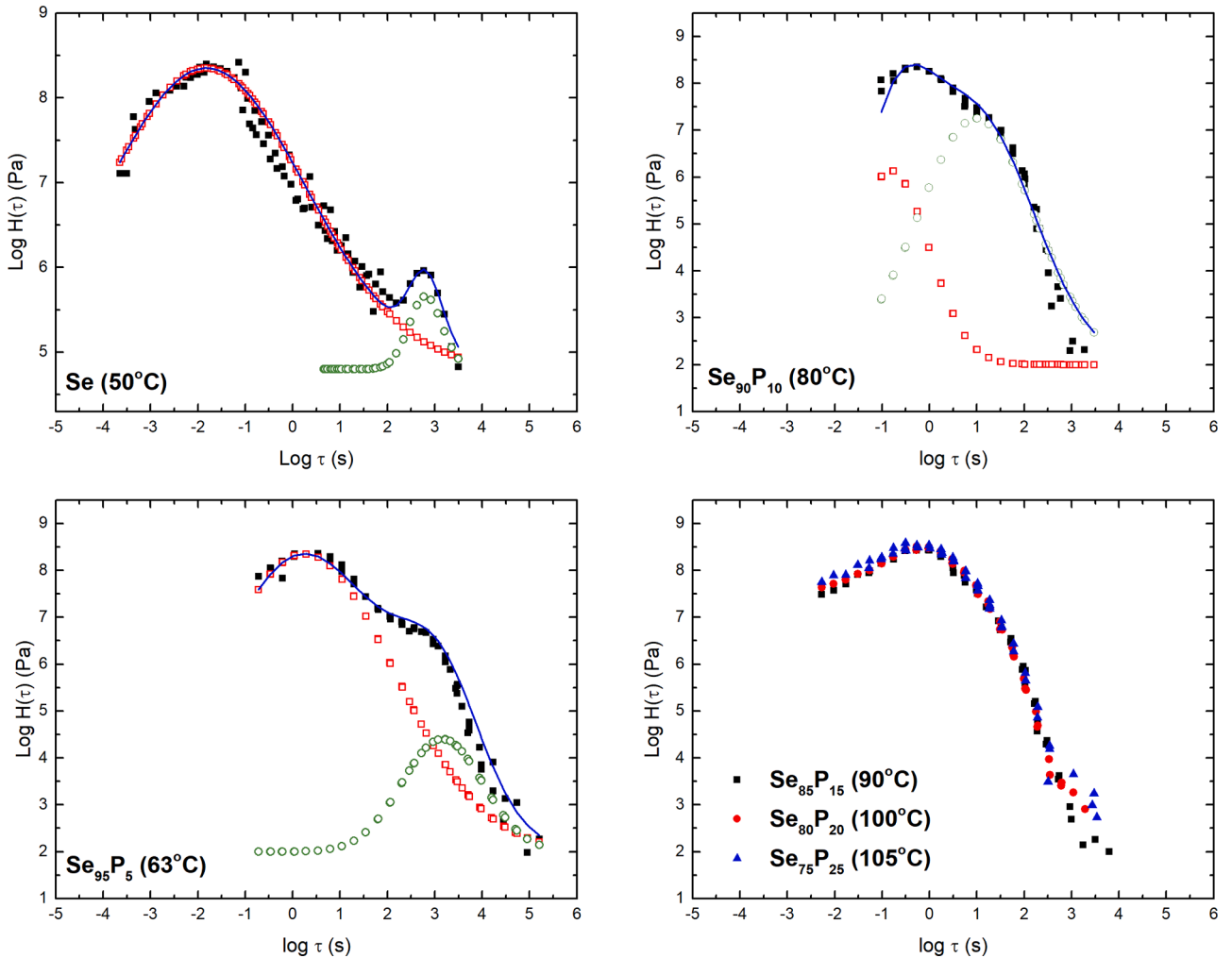

Fig. 6. Relaxation spectra H(τ) of P_xSe_{100-x} supercooled liquids. Filled squares are experimental data. Empty squares and circles represent the Gaussian fitting of the fast and slow processes, respectively. Solid lines represent the total fit to the experimental data. Data for pure Se is taken from Zhu et al. [13].

comparing the rheological behavior of high-Se liquids with different cross-linkers, namely P, Ge and As. Such a comparison between the G′(ω), G″(ω) and H(τ) spectra of P$_5$Se$_{95}$, Ge$_4$Se$_{96}$ and As$_5$Se$_{95}$ liquids with similar Se chain length and at nearly iso-viscous ($\sim 10^9$ Pa s) temperature is shown in Fig. 7. The G′(ω) and G″(ω) data for the Ge$_4$Se$_{96}$ and As$_5$Se$_{95}$ liquids are taken from a previous study [3,5]. The most noteworthy feature in these spectra is the difference in the separation of the timescale between the fast segmental chain motion and the slow bond scission/renewal dynamics, which is significantly smaller in the P-Se liquid compared to its Ge or As counterparts. This result suggests that the temporal coupling between the two relaxation mechanisms is the strongest in the P-Se system. As mentioned above, such a strong coupling may originate from the presence of the unique speciation equilibria in this system, exemplified by Eqs. (1) and ((2) that require the

involvement and rearrangement of the Se chain segments in the inter-conversion between Se=P(Se$_{1/2}$)$_3$ or P$_2$(Se$_{1/2}$)$_4$ and P(Se$_{1/2}$)$_3$ units. Moreover, while the FWHM of the fast process in the H(τ) spectra is similar in all cases, that of the slow process (~ 0.86 log units) for the P$_5$Se$_{95}$ liquid is much larger than that for the Ge$_4$Se$_{96}$ and As$_5$Se$_{95}$ liquids (~ 0.56 log units). The similar FWHM for the chain dynamics in all three liquids is not surprising considering the fact that they all have similar Se chain lengths. On the other hand, as noted above, the P$_5$Se$_{95}$ liquid is characterized by a wider variety of bonding and structural moieties compared to its As and Ge analogues, which are characterized by either Ge-Se or As-Se bonds and either GeSe$_{4/2}$ tetrahedra or AsSe$_{3/2}$ pyramids. This is consistent with the significantly larger FWHM for the bond scission/renewal dynamics in the H(τ) spectrum of the P$_5$Se$_{95}$ liquid compared to those for the Ge$_4$Se$_{96}$ and As$_5$Se$_{95}$ liquids.
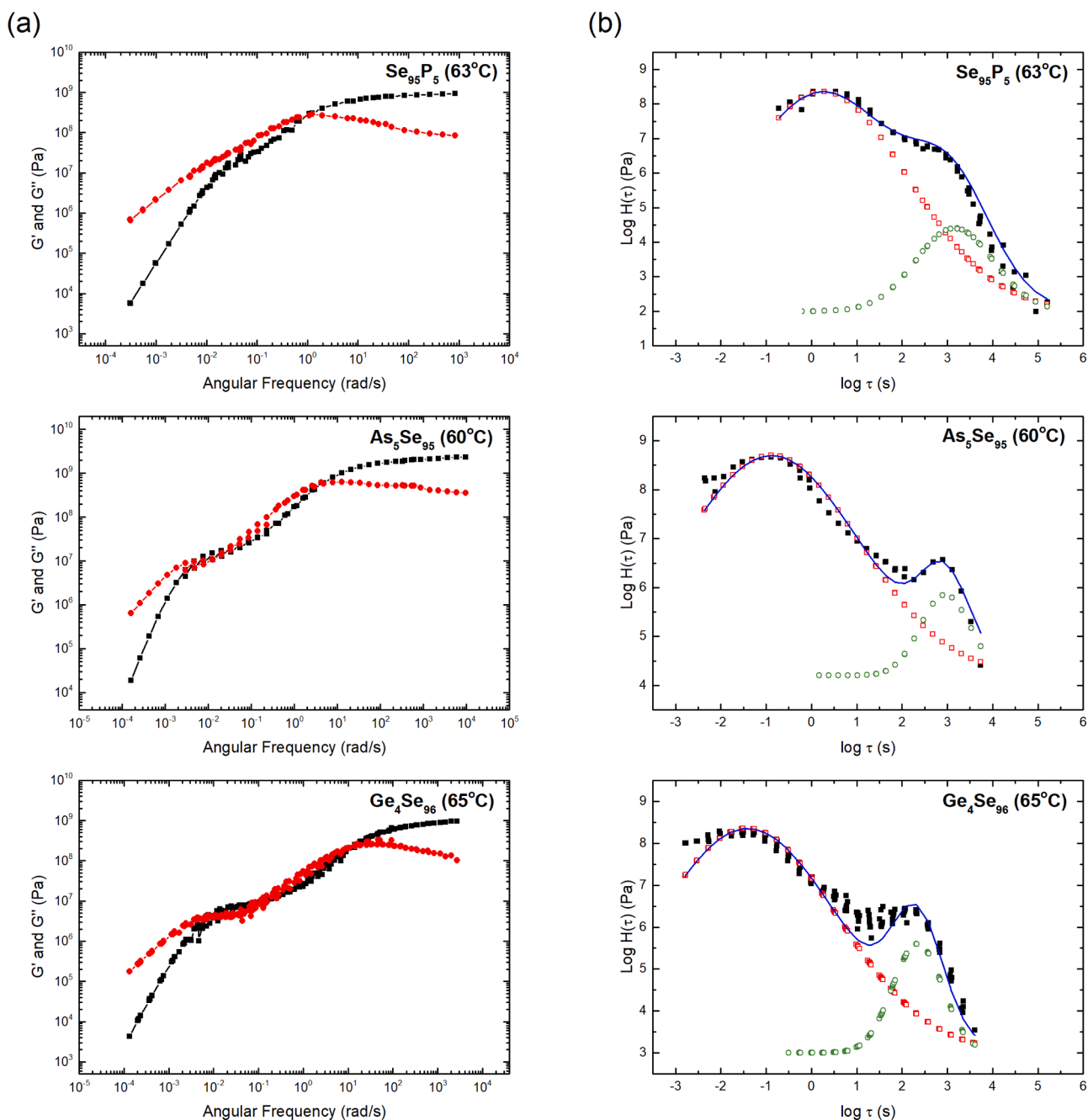
Fig. 7. Comparisons between binary P$_5$Se$_{95}$, Ge$_4$Se$_{96}$ [3] and As$_5$Se$_{95}$ [5] supercooled liquids with similar [Se]$_n$ chain length of (a) master curves of G′ (squares), G″ (circles) and (b) relaxation spectra H(τ). The symbols in (b) have the same meaning as in Fig. 6.

4. Conclusions

The structure of binary P_xSe_{100-x} ($0 \leq x \leq 25$) glasses is characterized by $[Se]_n$ chain segments that are cross-linked by $PSe_{3/2}$ pyramids, Se=P $(Se_{1/2})_3$ tetrahedra and ethylene-like $_{2/2}SeP\text{-}PSe_{2/2}$ structural units. The structural evolution is consistent with the corresponding variation in isothermal viscosity, glass transition temperature T_g and fragility m. Similar to their counterparts in the As-Se and Ge-Se systems, the $G'(\omega)$ and $G''(\omega)$ data for the Se-rich P_xSe_{100-x} liquids with $x \leq 10$ display the presence of two relaxation processes, namely fast segmental Se chain motion and slow bond scission/renewal dynamics. The corresponding relaxation spectra $H(\tau)$ indicate that the distribution of the relaxation timescale for chain dynamics is closely related to the Se chain length, whereas that for bond scission/renewal is controlled by the variety of the bond types and structural moieties involved in the process. Inspection of the $H(\tau)$ spectra indicate that these two dynamical processes are more strongly coupled in P-Se liquids, compared to their As-Se and Ge-Se counterparts with similar Se chain lengths. This unique behavior of P-Se liquids is likely due to the causal relationship between the chemical exchange between the Se=P$(Se_{1/2})_3$ or $P_2(Se_{1/2})_4$ and $P(Se_{1/2})_3$ units and the segmental motion of the Se chains. Finally, the segmental chain dynamics disappear in liquids with $x \geq 15$ as the Se chain length becomes too short to sustain such motion.

Author statement

Bing Yuan: All experimental measurements, data processing and interpretation, manuscript writing. Sabyasachi Sen: Conceived the project, provided supervision and wrote part the manuscript. Bruce Aitken: Glass synthesis, project supervision and manuscript editing.

Declaration of Competing Interest

The authors declare that they have no known competing financial interests or personal relationships that could have appeared to influence the work reported in this paper.

Acknowledgement

References

[1] B.G. Aitken, S.C. Currie, B.C. Monahan, L.-M. Wu, E.W. Coonan, Chalcogenide glass for low viscosity extrusion and injection molding, US 7116888 B1, 2006.

[2] Q. Zheng, J.C. Mauro, Viscosity of glass-forming systems, J. Am. Ceram. Soc. 100 (2017) 6–25.

[3] S. Sen, Y. Xia, W. Zhu, M. Lockhart, B. Aitken, Nature of the floppy-to-rigid transition in chalcogenide glass-forming liquids, J. Chem. Phys. 150 (2019), 144509.

[4] W. Zhu, B.G. Aitken, S. Sen, Communication: observation of ultra-slow relaxation in supercooled selenium and related glass-forming liquids, J. Chem. Phys. 148 (2018), 111101.

[5] W. Zhu, B. Aitken, S. Sen, Investigation of the shear relaxation behavior of As-Se liquids within the framework of entropic and elastic models of viscous flow, J. Non. Cryst. Solids 534 (2020), 119959.

[6] B. Yuan, B. Aitken, S. Sen, Rheology of supercooled Se-Te chain liquids: role of Te as an interchain cross-linker, J. Non. Cryst. Solids 529 (2020), 119764.

[7] W. Zhu, M.J. Lockhart, B.G. Aitken, S. Sen, Rheology of the λ transition in liquid sulfur: insights from arsenic sulfide liquids, J. Chem. Phys. 148 (2018), 244506.

[8] M. Marple, J. Badger, I. Hung, Z. Gan, K. Kovnir, S. Sen, Structure of amorphous selenium by 2D ^{77}Se NMR spectroscopy: an end to the dilemma of chain versus ring, Angew. Chemie 129 (2017) 9909–9913.

[9] G. Yang, B. Bureau, T. Rouxel, Y. Gueguen, O. Gulbiten, C. Roiland, E. Soignard, J. L. Yarger, J. Troles, J.C. Sanglebeouf, P. Lucas, Correlation between structure and physical properties of chalcogenide glasses in the As$_x$Se$_{1-x}$ system, Phys. Rev. B 82 (2010), 195206.

[10] T.G. Edwards, S. Sen, E.L. Gjersing, A combined ^{77}Se NMR and Raman spectroscopic study of the structure of Ge$_x$Se$_{1-x}$ glasses: towards a self consistent structural model, J. Non. Cryst. Solids 358 (2012) 609–614.

[11] E.L. Gjersing, S. Sen, Structure, connectivity, and configurational entropy of Ge$_x$Se$_{100-x}$ glasses: results from ^{77}Se MAS NMR spectroscopy, J. Phys. Chem. C 114 (2010) 8601–8608.

[12] W. Zhu, I. Hung, Z. Gan, B. Aitken, S. Sen, Dynamical processes related to viscous flow in a supercooled arsenic selenide glass-forming liquid: results from high-temperature ^{77}Se NMR spectroscopy, J. Non. Cryst. Solids 526 (2019), 119698.

[13] W. Zhu, B.G. Aitken, S. Sen, Observation of a dynamical crossover in the shear relaxation processes in supercooled selenium near the glass transition, J. Chem. Phys. 150 (2019), 094502.

[14] Z.U. Borisova, Glassy Semiconductors, Springer US, 1981.

[15] D.G. Georgiev, M. Mitkova, P. Boolchand, G. Brunklaus, H. Eckert, M. Micoulaut, Molecular structure, glass transition temperature variation, agglomeration theory, and network connectivity of binary P-Se glasses, Phys. Rev. B 64 (2001), 134204.

[16] A. Bytchkov, F. Fayon, D. Massiot, L. Hennet, D.L. Price, ^{31}P solid-state NMR studies of the short-range order in phosphorus-selenium glasses, Phys. Chem. Chem. Phys. 12 (2010) 1535–1542.

[17] R.T. Phillips, M.K. Ellis, Microstructure of P-Se glasses and low frequency Raman scattering, J. Non. Cryst. Solids 164–166 (1993) 135–138.

[18] D. Lathrop, H. Eckert, Quantitative determination of the structural units in phosphorus-selenium glasses by ^{31}P dipolar and magic-angle-spinning NMR spectroscopy, Phys. Rev. B 43 (1991) 7279–7287.

[19] D. Lathrop, H. Eckert, Dipolar NMR spectroscopy of nonoxidic glasses. structural characterization of the system phosphorus-selenium by ^{31}P-^{77}Se spin echo double resonance NMR, J. Am. Chem. Soc. 112 (1990) 9017–9019.

[20] D. Lathrop, H. Eckert, Chemical disorder in non-oxide chalcogenide glasses. Site speciation in the system phosphorus-selenium by magic angle spinning NMR at very high spinning speeds, J. Phys. Chem. 93 (1989) 7895–7902.

[21] D. Lathrop, H. Eckert, NMR studies of chalcogenide glasses: the system phosphorus-selenium, J. Non. Cryst. Solids 106 (1988) 417–420.

[22] R. Maxwell, H. Eckert, Molten-state kinetics in glass-forming systems. A high-temperature NMR study of the system phosphorus-selenium, J. Phys. Chem. 99 (1995) 4768–4778.

[23] R. Maxwell, H. Eckert, Speciation equilibria, clustering, and chemical-exchange kinetics in non-oxide glasses and melts. high-temperature ^{31}P NMR study of the system phosphorus-selenium, J. Am. Chem. Soc. 115 (1993) 4747–4753.

[24] R. Maxwell, H. Eckert, Chemical equilibria in glass-forming melts: high-temperature ^{31}P and ^{77}Se NMR of the phosphorus-selenium system, J. Am. Chem. Soc. 116 (1994) 682–689.

[25] S.N. Yannopoulos, K.S. Andrikopoulos, Raman scattering study on structural and dynamical features of noncrystalline selenium, J. Chem. Phys. 121 (2004) 4747–4758.

[26] Z. Borisova, B. Kasatkin, E. Kim, Izv. Akad. Nauk SSSR Neorg. Mater. 9 (1973) 822.

[27] F. Heyder, D. Linke, Z. Chem. 13 (1973) 480.

[28] R. Blachnik, A. Hoppe, Glass transition and specific heats in the systems P-S, P-Se, As-S and As-Se, J. Non. Cryst. Solids 34 (1979) 191–201.

[29] Y. Monteil, H. Vincent, Z. Anorg. Allg. Chem. 416 (1975) 181.

[30] E.I. Kim, G.M. Orlova, Viscosity of glasses in the P-Se system, J. Appl. Chem. USSR 47 (1974), 1081–1021.

[31] J.C. Mauro, Y. Yue, A.J. Ellison, P.K. Gupta, D.C. Allan, Viscosity of glass-forming liquids, Proc. Natl. Acad. Sci. 106 (2009) 19780–19784.

[32] C. Zhang, L. Hu, Y. Yue, J.C. Mauro, Fragile-to-strong transition in metallic glass-forming liquids, J. Chem. Phys. 133 (2010), 014508.

[33] C. Gainaru, R. Figuli, T. Hecksher, B. Jakobsen, J.C. Dyre, M. Wilhelm, R. Böhmer, Shear-modulus investigations of monohydroxy alcohols: evidence for a short-chain-polymer rheological response, Phys. Rev. Lett. 112 (2014), 098301.

[34] N. Lou, Y. Wang, X. Li, H. Li, P. Wang, C. Wesdemiotis, A.P. Sokolov, H. Xiong, Dielectric relaxation and rheological behavior of supramolecular polymeric liquid, Macromolecules 46 (2013) 3160–3166.

[35] J.D. Ferry, Viscoelastic Properties of Polymers, John Wiley & Sons, 1980.

[36] P. Koštál, J. Málek, Viscosity of Se-Te glass-forming system, Pure Appl. Chem. 87 (2015) 239–247.